AMERICAN SOCIETY FOR MICROBIOLOGY | Journal of Virology®

GENOME REPLICATION AND REGULATION OF VIRAL GENE EXPRESSION

The C Protein Is Recruited to Measles Virus Ribonucleocapsids by the Phosphoprotein

Christian K. Pfaller,[a,b] Louis-Marie Bloyet,[c*] Ryan C. Donohue,[a,d] Amanda L. Huff,[a,d] William P. Bartemes,[a,d] Iris Yousaf,[a,d] Erica Urzua,[c] Mathieu Clavière,[c] Marie Zachary,[c] Valentin de Masson d'Autume,[c] Sandra Carson,[a,d] Adam J. Schieferecke,[a,d] Alyssa J. Meyer,[a,d] Denis Gerlier,[c] Roberto Cattaneo[a,d]

[a]Department of Molecular Medicine, Mayo Clinic, Rochester, Minnesota, USA
[b]Division of Veterinary Medicine, Paul-Ehrlich-Institut, Langen, Germany
[c]Centre International de Recherche en Infectiologie, CIRI, INSERM, U1111, CNRS, UMR5308, Université Claude Bernard Lyon 1, ENS Lyon, Univ Lyon, Lyon, France
[d]Virology and Gene Therapy Program, Mayo Clinic Graduate School of Biomedical Sciences, Rochester, Minnesota, USA

ABSTRACT Measles virus (MeV), like all viruses of the order *Mononegavirales*, utilizes a complex consisting of genomic RNA, nucleoprotein, the RNA-dependent RNA polymerase, and a polymerase cofactor, the phosphoprotein (P), for transcription and replication. We previously showed that a recombinant MeV that does not express another viral protein, C, has severe transcription and replication deficiencies, including a steeper transcription gradient than the parental virus and generation of defective interfering RNA. This virus is attenuated *in vitro* and *in vivo*. However, how the C protein operates and whether it is a component of the replication complex remained unclear. Here, we show that C associates with the ribonucleocapsid and forms a complex that can be purified by immunoprecipitation or ultracentrifugation. In the presence of detergent, the C protein is retained on purified ribonucleocapsids less efficiently than the P protein and the polymerase. The C protein is recruited to the ribonucleocapsid through its interaction with the P protein, as shown by immunofluorescence microscopy of cells expressing different combinations of viral proteins and by split luciferase complementation assays. Forty amino-terminal C protein residues are dispensable for the interaction with P, and the carboxyl-terminal half of P is sufficient for the interaction with C. Thus, the C protein, rather than being an "accessory" protein as qualified in textbooks so far, is a ribonucleocapsid-associated protein that interacts with P, thereby increasing replication accuracy and processivity of the polymerase complex.

IMPORTANCE Replication of negative-strand RNA viruses relies on two components: a helical ribonucleocapsid and an RNA-dependent RNA polymerase composed of a catalytic subunit, the L protein, and a cofactor, the P protein. We show that the measles virus (MeV) C protein is an additional component of the replication complex. We provide evidence that the C protein is recruited to the ribonucleocapsid by the P protein and map the interacting segments of both C and P proteins. We conclude that the primary function of MeV C is to improve polymerase processivity and accuracy, rather than uniquely to antagonize the type I interferon response. Since most viruses of the *Paramyxoviridae* family express C proteins, their primary function may be conserved.

KEYWORDS measles virus, replication, processivity, C protein, ribonucleocapsid, replicase, RNA synthesis, phosphoprotein, large protein, polymerase

Replication of nonsegmented negative-strand RNA viruses (order *Mononegavirales*) principally relies on two components: the viral nucleocapsid consisting of viral genomic RNA enwrapped by the nucleocapsid protein (or "nucleoprotein" [N]) and the

Citation Pfaller CK, Bloyet L-M, Donohue RC, Huff AL, Bartemes WP, Yousaf I, Urzua E, Clavière M, Zachary M, de Masson d'Autume V, Carson S, Schieferecke AJ, Meyer AJ, Gerlier D, Cattaneo R. 2020. The C protein is recruited to measles virus ribonucleocapsids by the phosphoprotein. J Virol 94:e01733-19. https://doi.org/10.1128/JVI.01733-19.

Editor Rebecca Ellis Dutch, University of Kentucky College of Medicine

Address correspondence to Christian K. Pfaller, Christian.Pfaller@pei.de, or Roberto Cattaneo, Cattaneo.Roberto@mayo.edu.

* Present address: Louis-Marie Bloyet, Microbiology and Immunobiology Department, Harvard Medical School, Boston, Massachusetts, USA.

Received 8 October 2019
Accepted 8 November 2019
Accepted manuscript posted online 20 November 2019
Published 31 January 2020

viral polymerase complex consisting of an RNA-dependent RNA polymerase (RdRp, or "large protein" [L]) and a cofactor (usually called phosphoprotein [P]) which mediates interaction between nucleocapsid and polymerase (1, 2). The genome is composed of a 3′ promoter region (called the "leader") preceding sequential transcription units separated by intergenic regions and followed by the complementary sequence of the antigenomic promoter (called the "trailer").

The polymerase is responsible for transcription, polyadenylation, capping, and methylation of mRNA and for synthesis of full-length viral genomic RNA. Initiation of both transcription and replication occurs exclusively at the 3′-leader and trailer sequences. Transcription occurs immediately after infection of a host cell and generates a gradient of mRNAs, with the genes proximal to the leader being the most abundantly transcribed and the genes most distal to the leader being transcribed at the lowest levels (1). This transcription gradient is based on lower processivity of the viral polymerase at each intergenic region. At later stages of infection, the polymerase switches into replication mode, which is characterized by high processivity leading to the generation of encapsidated full-length antigenomic and genomic RNA.

We have previously shown that in the case of measles virus (MeV), a member of the *Paramyxoviridae* family (genus *Morbillivirus*), processivity of replication relies on another viral factor, the C protein, which is encoded in an alternative open reading frame of the *P* gene (3): a recombinant MeV lacking C protein expression (C "knockout," MeV-C^{KO}) frequently generates copyback-defective interfering (DI) RNA (4). Copyback-DI RNA are replicative chimeric RNAs combining positive (+) and negative (−) genomic RNAs. They can form immunostimulatory double-stranded RNAs (dsRNAs) which then activate protein kinase R (PKR)-mediated, melanoma differentiation-associated gene 5 (MDA-5)-mediated, and retinoic acid inducible gene-I (RIG-I)-mediated innate immune responses (5–7), resulting in strong attenuation of MeV-C^{KO} *in vitro* (8, 9), in human primary peripheral blood mononuclear cells (10), and *in vivo* (9, 11). In addition, MeV-C^{KO} exhibits a steeper transcription gradient than a C protein-expressing MeV (5). Generation of DI RNA and a steeper transcription gradient suggest that the C protein improves the processivity of the MeV polymerase. Moreover, results of minigenome assay-based studies suggest that C protein regulates genome synthesis (12–14).

Here, we asked whether the MeV C protein is a component of the viral replication complex. After analyzing C protein localization by confocal immunofluorescence, we studied its interaction with the viral replication complex by immunoprecipitation (IP) and density gradient centrifugation. We biochemically identified the interaction partner of C protein within the ribonucleoprotein (RNP) complex. We conclude that the C protein is a component of the replication complex that enhances polymerase processivity.

RESULTS

MeV C protein colocalizes with replication bodies. MeV replication occurs in defined cytoplasmic inclusion bodies, also known as replication bodies (5, 15, 16). To assess C protein localization, we infected HeLa cells with a standard MeV expressing green fluorescent protein [GFP; vac2(GFP)] or with a C-deficient MeV [C^{KO}(GFP)] and analyzed colocalization of viral P, L, and C proteins with N protein at 48 h postinfection (Fig. 1). As shown previously (15), N and P colocalize in large cytoplasmic replication bodies (Fig. 1A) that also contain L protein (Fig. 1B). C protein also accumulates in these bodies and is additionally found in the nuclei of infected cells (Fig. 1C), as reported previously (17). The absence of C signal in C^{KO}(GFP)-infected cells indicated the specificity of the anti-C antibody. In contrast, the viral transmembrane glycoprotein hemagglutinin (H) was not included in viral replication bodies (Fig. 1D). Thus, the C protein colocalizes with replication bodies.

C protein and viral RNPs coimmunoprecipitate. We next asked whether C protein is associated with the viral replication complex. For this, we generated a recombinant MeV expressing carboxy-terminally 3×FLAG-tagged C protein (C^{FL}) as well as amino-terminally HA-tagged L protein (^{HA}L). We named this virus vac2-2tags (Fig. 2A). This

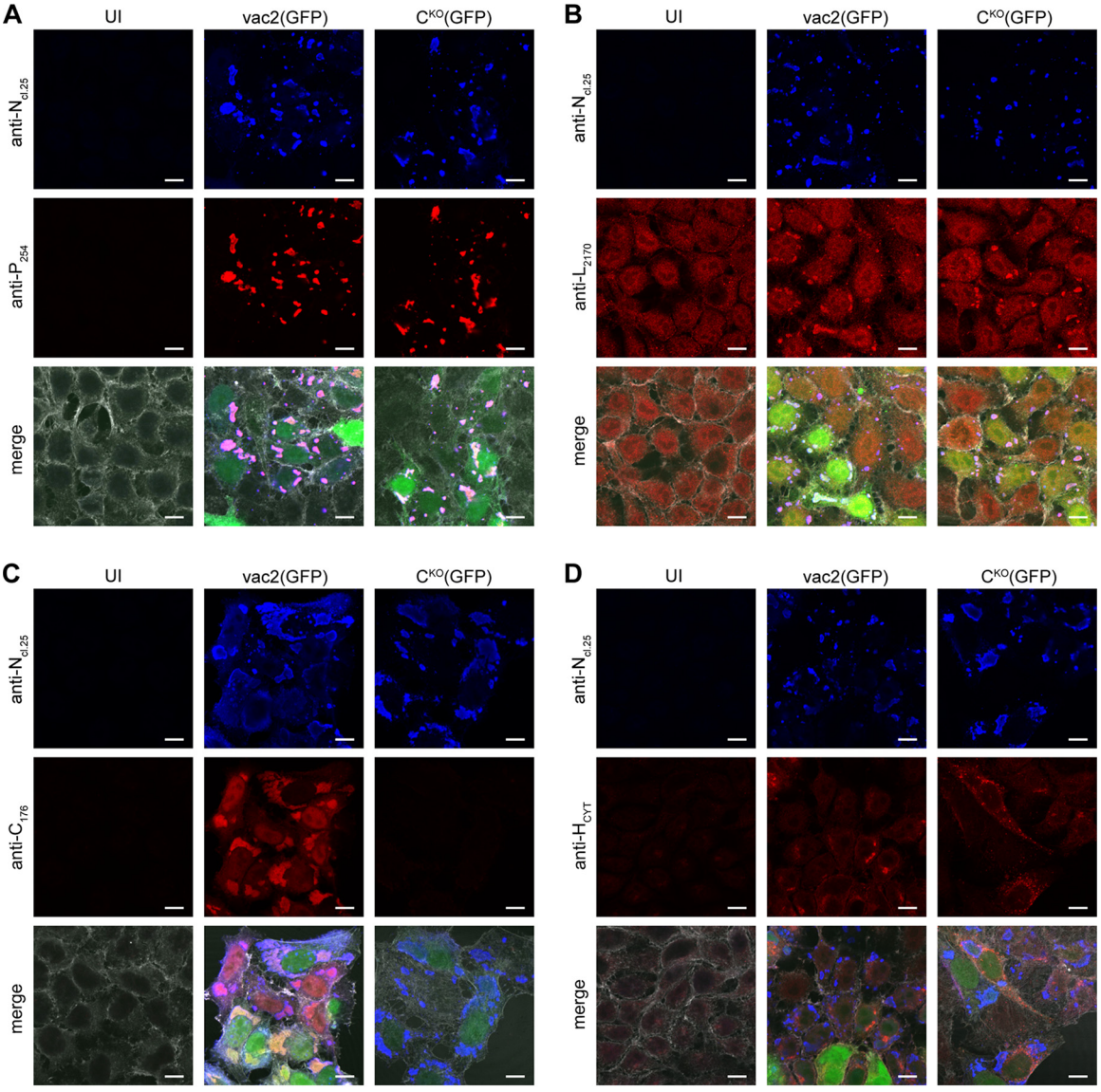

FIG 1 C protein colocalizes with components of the MeV replication complex. Immunofluorescence staining of HeLa cells infected with vac2(GFP), cells infected with C^{KO}(GFP), and uninfected (UI) cells was performed. (A) Costaining of N (blue) and P (red). (B) Costaining of N (blue) and L (red). Uninfected cells show diffuse unspecific staining with anti-L. Infected cells in addition show concentration of L signal in viral inclusion bodies. (C) Costaining of N (blue) and C (red). (D) Costaining of N (blue) and H (red). Merge panels include signals for GFP (green) and actin (gray). The antibodies used are indicated on the left of each row of panels. Bar, 10 μm.

virus expresses C^{FL} from an additional transcription unit instead of from its original location in the *P/V/C* gene, preserving the P/V open reading frame. An untagged virus (vac2-notags) was generated as a control (Fig. 2A). Both viruses reached titers similar to those seen with the parental vac2(GFP) strain.

We then infected HeLa cells with the two viruses, prepared cell lysates at 48 h postinoculation, and immunoprecipitated protein complexes using anti-FLAG-coated or anti-N-coated magnetic beads. The precipitates were then analyzed by Western blotting (Fig. 2B). The infection levels of the two viruses were slightly different, leading to reduced viral protein expression of vac2-notags compared to vac2-2tags (Fig. 2B, lanes 2 and 3). C^{FL}, but not untagged C, was efficiently precipitated using anti-FLAG beads (Fig. 2B, lanes 5 and 6). The sample derived from vac2-2tags (lane 6), but not that derived from vac2-notags (lane 5), contained viral N, P, and L proteins, indicating an interaction (direct or indirect) of the RNP with C^{FL} rather than unspecific binding to the beads. In contrast, immunoprecipitation of N protein resulted in coprecipitation of C

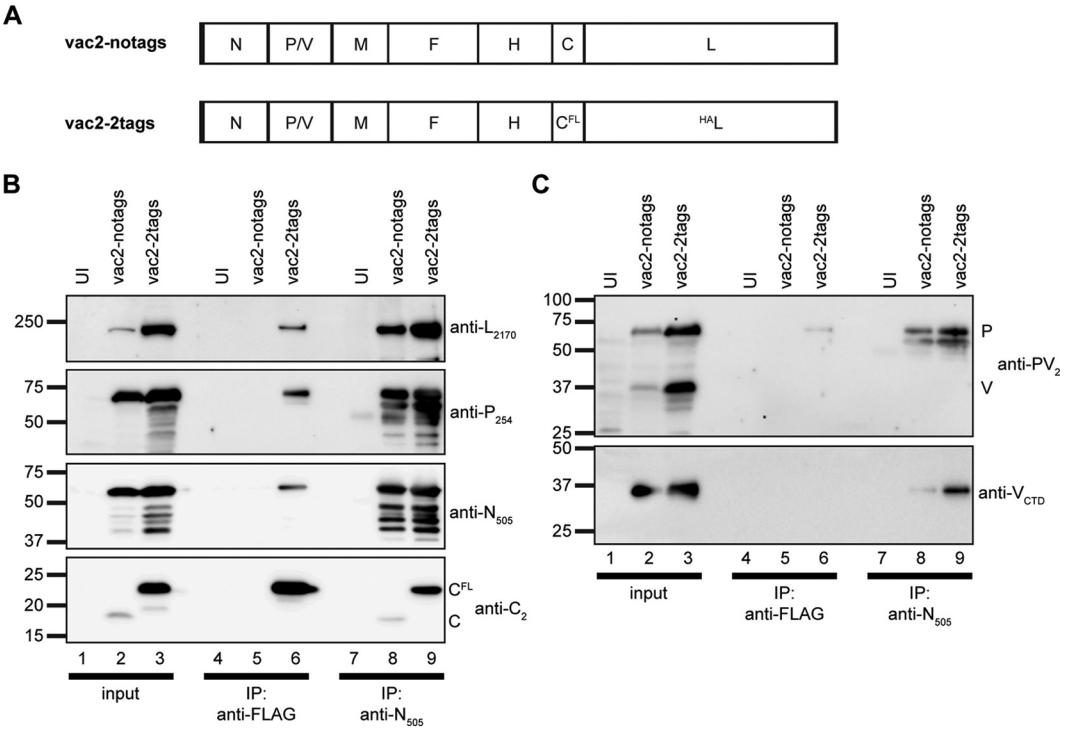

FIG 2 Analysis of the C protein interactions by coimmunoprecipitation. (A) Genomes of the viruses generated for this and subsequent experiments. vac2-notags expresses the standard C protein from an additional transcription unit located downstream of the H gene; vac2-2tags expresses a 3×FLAG-tagged C protein (C^{FL}) from an additional transcription unit located downstream of the H gene; the L protein of this virus is tagged with an HA epitope (^{HA}L). (B) Western blot analysis of uninfected (UI) cell lysates and of cells infected with the viruses indicated at the top. Analyses were performed before (input) and after IP using anti-FLAG-coated or anti-N_{505}-coated beads, as indicated on the bottom. The four specific antisera used are indicated on the right of each panel, and molecular weight markers are indicated on the left. IP samples are concentrated 10-fold over the input lysates. (C) Western blot analyses using antiserum recognizing P and V (anti-PV_2) or a V-specific antiserum (anti-V_{CTD}).

and C^{FL} in addition to P and L proteins (Fig. 2B, lanes 8 and 9), indicating that the FLAG tag is not required for binding of C to the viral RNP.

In contrast, V protein, which shares its amino-terminal protein sequence with P (amino acids 1 to 231) but has a unique carboxy terminus (18), did not coprecipitate with C^{FL} (Fig. 2C, lane 6). The absence of V protein was confirmed by probing with two antisera recognizing either the shared P/V amino terminus or the V-specific carboxy terminus. We detected a band of V protein in anti-N immunoprecipitates (Fig. 2C, lanes 8 and 9), indicating that V may interact with free N protein via its amino terminus (that is common with P) and binds to the core of N in N^{0}P complex (19, 20).

C protein copurifies with viral nucleocapsids. We next asked whether the interaction between C and the viral RNP is primarily mediated through the nucleocapsid (N-RNA) or through the viral polymerase complex (L-P). For this, we extracted nucleocapsids of vac2-2tags or vac2(GFP) viruses from infected HeLa cells and purified them through CsCl-density gradient ultracentrifugation (21, 22). CsCl gradients were prepared with increasing amounts of the detergent sarkosyl, which disrupts the interaction of L-P with N-RNA, resulting in "stripped" nucleocapsids with higher density (22). As anticipated, the RNP band became denser and more compact with increasing amounts of sarkosyl (Fig. 3A, white bars).

Purified nucleocapsids were analyzed by SDS-PAGE and silver staining (Fig. 3B). A predominant band appeared at about 56 kDa (Fig. 3B, arrow), representing N protein as confirmed by Western blot analysis (Fig. 3C, third blot). Multiple additional proteins between 10 and 250 kDa copurified with RNPs. Increasing amounts of sarkosyl reduced the strength of these additional signals, consistent with stripping of weakly interacting proteins.

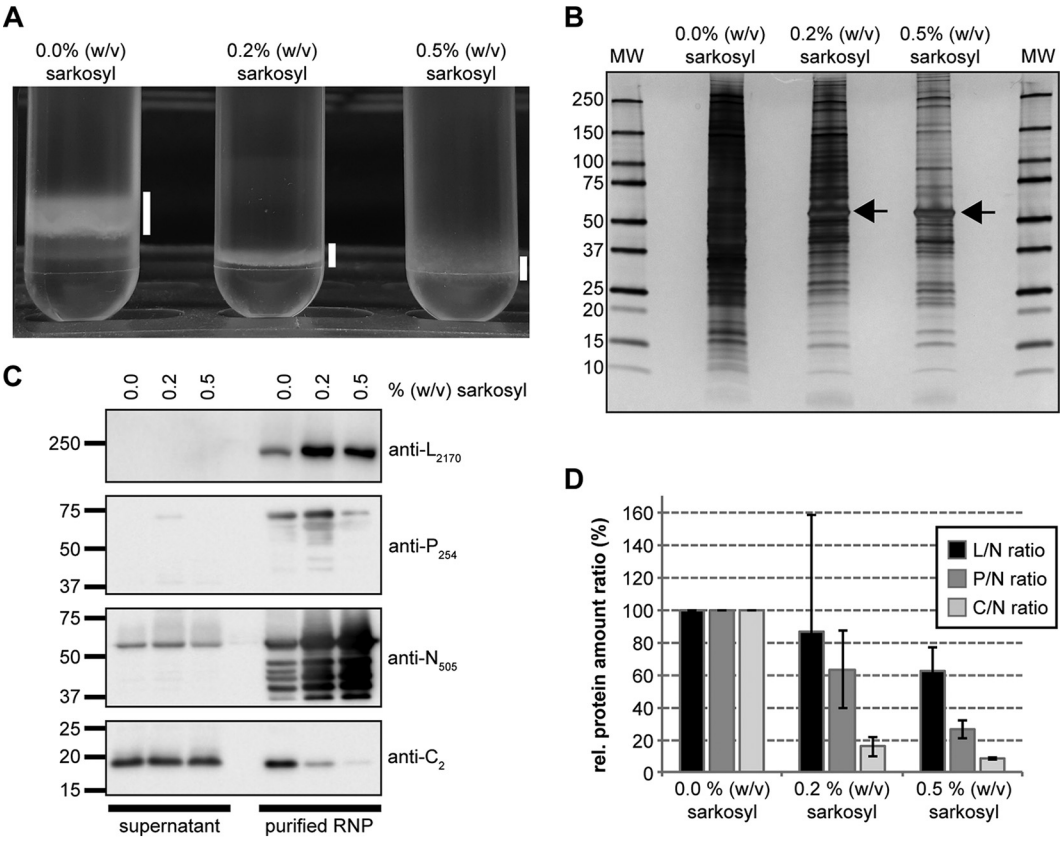

FIG 3 Viral proteins found in density gradient-purified MeV RNPs. (A) Nucleocapsid bands after centrifugation in CsCl gradients containing increasing amounts of the detergent sarkosyl. The amount of detergent is indicated at the top. White bars indicate locations of the RNPs at equilibrium, as harvested for further analysis. (B) Silver-stained SDS-PAGE of purified RNPs; MW, protein molecular weight standard. (C) Western blot analysis of supernatants and RNPs after CsCl density gradient separation. (D) Quantification of Western blot band intensities in (C). The diagram represents average values ± standard deviations of results from three independent experiments.

Western blot analysis of purified RNPs revealed the presence of N, P, L, and C proteins in the RNP samples (Fig. 3C). While N protein became more abundant with increasing sarkosyl concentrations due to the better solubilization of RNPs throughout the gradient/during gradient running (Fig. 3C) as already reported (22), P, L, and C proteins did not. Indeed, quantification of band intensities confirmed loss of the polymerase complex on RNPs with increasing sarkosyl concentrations (Fig. 3D). C protein was retained on RNPs even less efficiently than P and L proteins in the presence of detergent. The levels of N, P, and L were low to nearly undetectable in the supernatant fraction (the top fraction of the CsCl gradient), while C was more prominent in the supernatant than in the RNP fraction. Stripping of C protein from the RNP did not increase the levels of C in the supernatant fraction due to dilution of the released C protein into the large volume of this fraction (approximately 5 ml). This experiment confirmed a weak physical interaction of C with the RNP without identifying its interaction partner within the RNP.

P protein is required for recruitment of C to the viral RNP. We next asked which viral protein recruits C to the viral RNP. For this, we analyzed protein localization in transfected cells by immunofluorescence staining. P protein, when expressed alone, is diffusely distributed in the cytoplasm (Fig. 4A, top row). In contrast, N protein expressed by itself forms small inclusion bodies (Fig. 4A, middle row). These typically can be observed both in cytoplasm and nucleus (data not shown) (23). When coexpressed, N and P form large cytoplasmic inclusion bodies (Fig. 4A, bottom row) that are similar to the viral replication centers formed during infection (Fig. 4B, middle row).

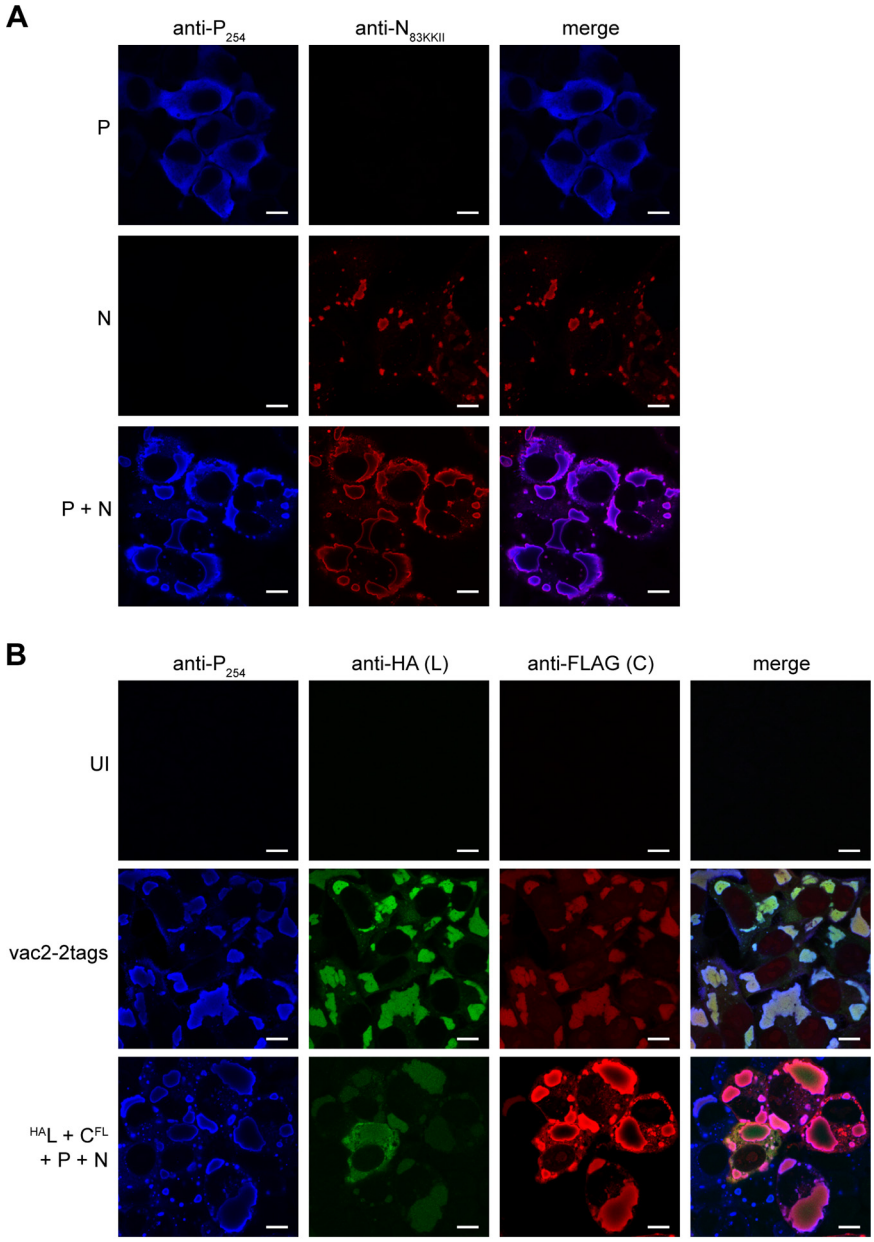

FIG 4 Immunofluorescence analyses of viral protein localization in transfected and infected cells. (A) Confocal immunofluorescence images of transfected HeLa cells. The expression plasmids used are indicated on the left of the panels and the antibodies used above the panels. Fluorophores on the secondary antibodies are indicated as follows: P, blue; N, red. (B) Confocal immunofluorescence images of uninfected (UI) cells, vac2-2tags-infected HeLa cells, or cells expressing N, P, C^{FL}, and ^{HA}L, as indicated on the left of the panels. The antibodies used are indicated above the panels. Fluorophores on the secondary antibodies are indicated as follows: P, blue; ^{HA}L, green, C^{FL}, red. Bar, 10 μm.

Using this assay of formation of inclusion bodies, we assessed the localization of C^{FL}. After coexpression, all four proteins colocalized in ways similar to those monitored in infected cells (Fig. 4B; compare bottom row with middle row). In the absence of P expression, neither C^{FL} nor ^{HA}L was recruited to N-containing inclusion bodies (Fig. 5A, middle and bottom rows). While C^{FL} was predominantly found in the nucleus, ^{HA}L remained in the cytoplasm. However, when P was coexpressed, ^{HA}L was efficiently recruited to the cytoplasmic inclusions (Fig. 5B, bottom row), confirming that P mediates the interaction of the viral nucleocapsid and the polymerase (24). Similarly, C^{FL} relocalized from the nucleus to the inclusion bodies in the presence of P (Fig. 5B, middle row).

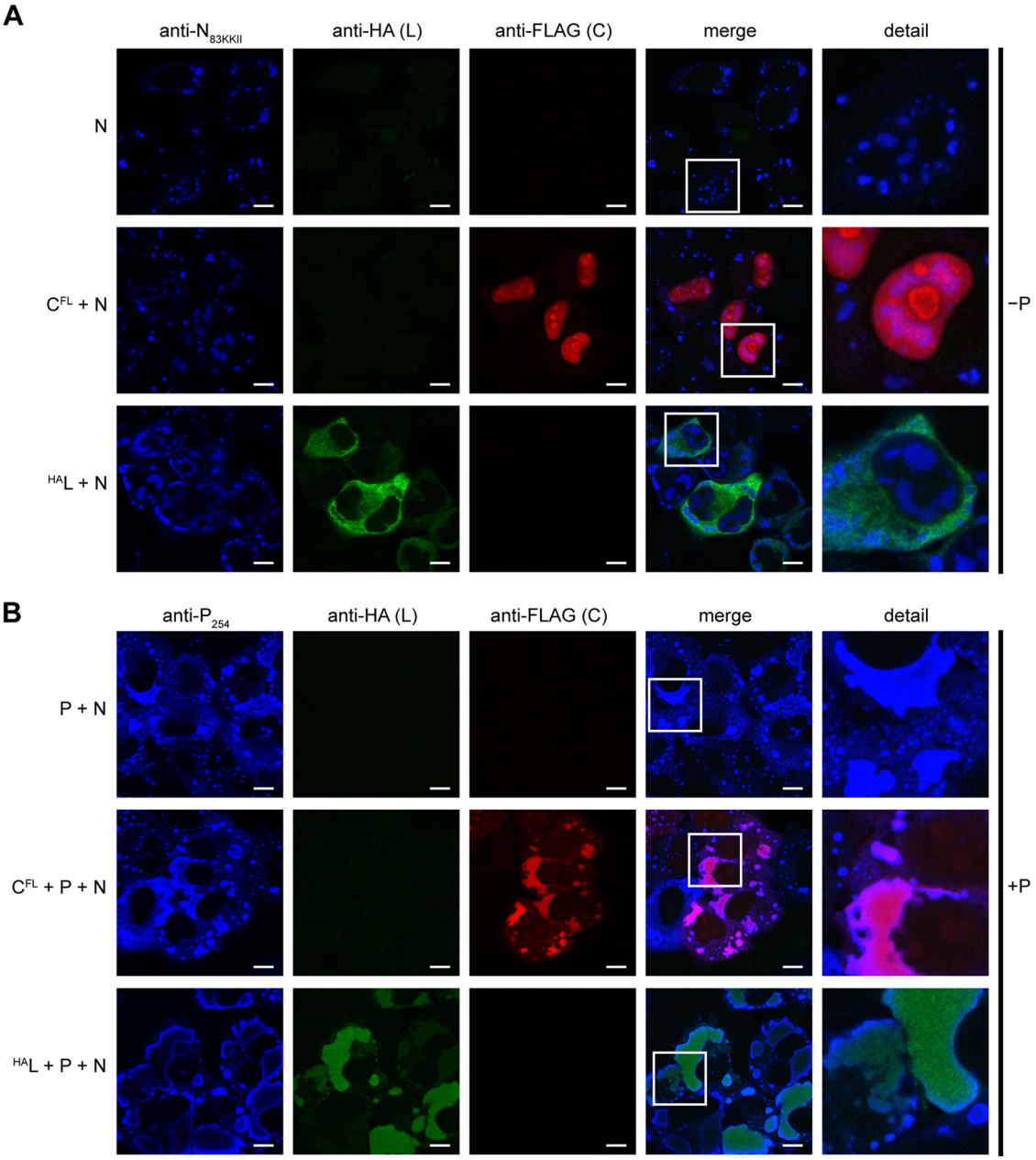

FIG 5 C protein requires P protein for relocalization to viral inclusion bodies. (A) Confocal immunofluorescence analysis of transient expression of N protein (top row), N and C^{FL} proteins (second row), or N and ^{HA}L proteins (bottom row). The antibodies used for staining are indicated at the top: N, blue; ^{HA}L, green; C^{FL}, red. "Merge" data represent a merger of the three staining antibodies. The last panel (detail) is an enlargement of the white box in the merge panel. Bar, 10 μm. (B) Confocal immunofluorescence analysis of transient expression of the same protein combinations, this time in the presence of P.

To verify that the P-C interaction was independent of the presence of N, we inserted the P protein into the outer mitochondrial membrane using a Tom20 tag (25, 26). We confirmed that, whereas untagged P had diffuse localization, Tom20-P was concentrated in cytoplasmic organelles shaped like mitochondria (Fig. 6, top two rows). FLAG-tagged L protein (^{FL}L) colocalized with mitochondrial Tom20-P (Fig. 6, middle two rows), and C^{FL} partially colocalized (Fig. 6, bottom two rows).

In a complementary approach to determine the interaction partner of C, we relied on a split *Gaussia* luciferase (glu) protein complementation assay that can detect weak protein-protein interactions (27) in the micromolar range (28). Indeed, the results of coimmunoprecipitation (Co-IP) experiments performed with cells expressing combina-

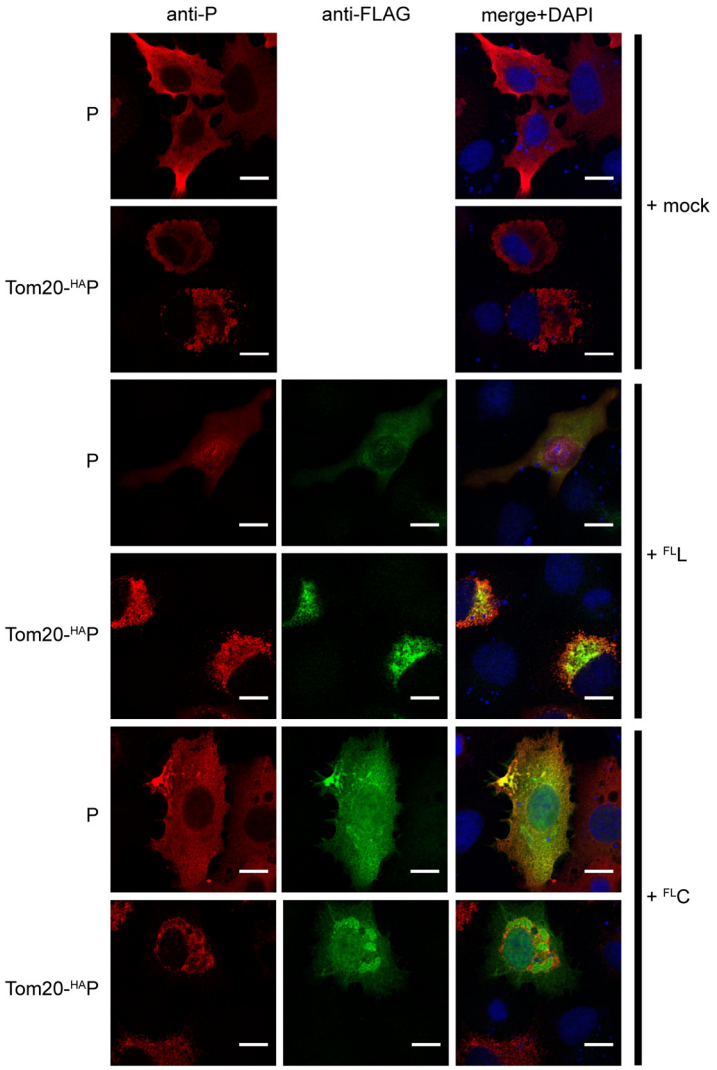

FIG 6 Colocalization of C and L proteins with mitochondrion-targeted P protein. Confocal immunofluorescence analysis of protein colocalization in transfected cells was performed. The P protein-variants (untagged P or Tom20-^{HA}P) expressed are indicated on the left. The coexpressed proteins are indicated on the right. At 24 h after transfection, BSR-T7 cells were fixed and P (red), ^{FL}L (green), Tom20-^{HA}P (red), and ^{FL}C (green) were immunolabeled. The right column shows merge pictures with DNA stained with DAPI. Bar, 10 μm.

tions of individual proteins were inconclusive, possibly because of the sensitivity of C interactions with RNP to detergent (Fig. 3C and D). Thus, we fused the split domains of glu (glu1 and glu2) to the amino or carboxy terminus of the viral proteins as described previously (29). To test protein-protein interactions, combinations of these constructs were coexpressed, and reconstitution of luciferase activity was quantified through bioluminescence. As expected, positive signals were observed for P-P and P-N coexpression (Fig. 7), confirming self-interaction of P (30) and N-P interaction (31, 32). P also interacted with a 620-amino-acid amino-terminal fragment of L (L_{1-620}) encompassing conserved regions I and II (24, 33, 34). Coexpression of P and C constructs reconstituted glu activity, but we did not observe luciferase complementation when C protein was coexpressed with N or L_{1-620} constructs (Fig. 7). This suggests that C interacts with P but not with N or L_{1-620}. In addition, C proteins fused to both glu domains reconstituted luciferase activity, suggesting C homo-oligomerization. Thus, the results of the split luciferase assays and the colocalization assays consistently indicated that C interacts with P but not with N or L.

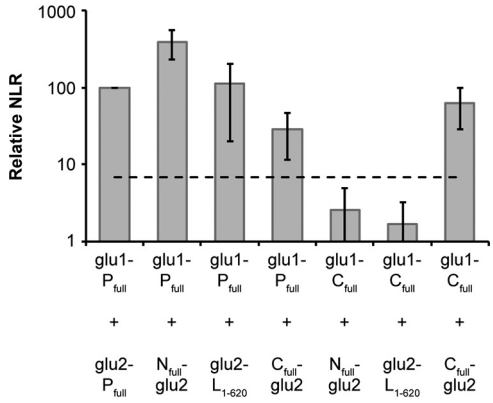

FIG 7 C protein interacts with P protein but not N or an L segment. *Gaussia* luciferase-based protein complementation assay. Interactions tested included P-P, P-N, P-L_{1-620}, P-C, C-N, C-L_{1-620}, and C-C (from left to right). Results represent the normalized luminescence ratio (NLR), shown as a percentage of the P-P interaction (vertical axis). The dashed line indicates the threshold above which an interaction is considered positive. The diagram represents average values ± standard deviations of results from three independent experiments.

Interacting segments of C and P. We then mapped the reciprocal binding sites between C and P proteins. Based on predicted secondary structure elements, the C reading frame was divided into four segments and fused to glu domains (Fig. 8A). We then assessed protein-protein interactions by a glu-protein complementation assay. Amino-terminal fragments C1 and C12 expressed alone were unable to interact with P, whereas addition of the C3 fragment (C123) partially restored binding (Fig. 8B). On the other hand, the fragment lacking only the C1 domain (C234) retained full binding activity, while additional amino-terminal truncation (C34 and C4) affected interaction with P strongly (Fig. 8C). Moreover, a C protein fragment encompassing the two central fragments (C23) retained about 40% binding activity compared to full-length C (Fig. 8C). Thus, the structured carboxy-terminal fragments (C234) are required and sufficient for P binding, while the unstructured amino-terminal fragment (C1) is dispensable. Our data suggest that the core binding domain of C to P is within the two central fragments (C23).This is in agreement with this region of C being well conserved among the members of the *Paramyxoviridae* family (35).

Similarly, based on available structural and functional information (19, 36), the P protein was divided into three regions, P1, P2, and P3 (residues 1 to 302, 303 to 374, and 375 to 507, respectively), and truncated P proteins were generated (Fig. 8D). Both the P2 and P3 segments were required for efficient C binding (Fig. 8E). The approximately 200 amino acids covered by P2 and P3 include the multimerization domain as well as regions of L and N binding (34, 37, 38) (Fig. 8D). These results reveal the interacting parts of the C and P proteins.

DISCUSSION

On the basis of observations made with another member of the *Paramyxoviridae* family, Sendai virus (SeV; also known as Murine parainfluenza virus), the C protein of paramyxoviruses was originally classified as nonstructural (39, 40). The fact that genetically engineered MeV and SeV knockout strains unable to express C proteins (C^{KO}) are viable in tissue culture later suggested that the C protein is an "accessory" protein (8, 11, 41–43). On the other hand, since the C proteins of SeV and MeV counteract different steps of innate immunity activation and interferon signaling (17, 44–48), they are considered interferon antagonists. In addition, several studies based on minireplicon assays showed that the C protein can restrict viral RNA synthesis (12, 13, 42, 49, 50), suggesting modulation of the viral RdRp activity. Consistent with this function, lack of C protein expression results in increased levels of viral double-stranded RNA and the generation of copyback-DI RNA (4, 5, 21, 51).

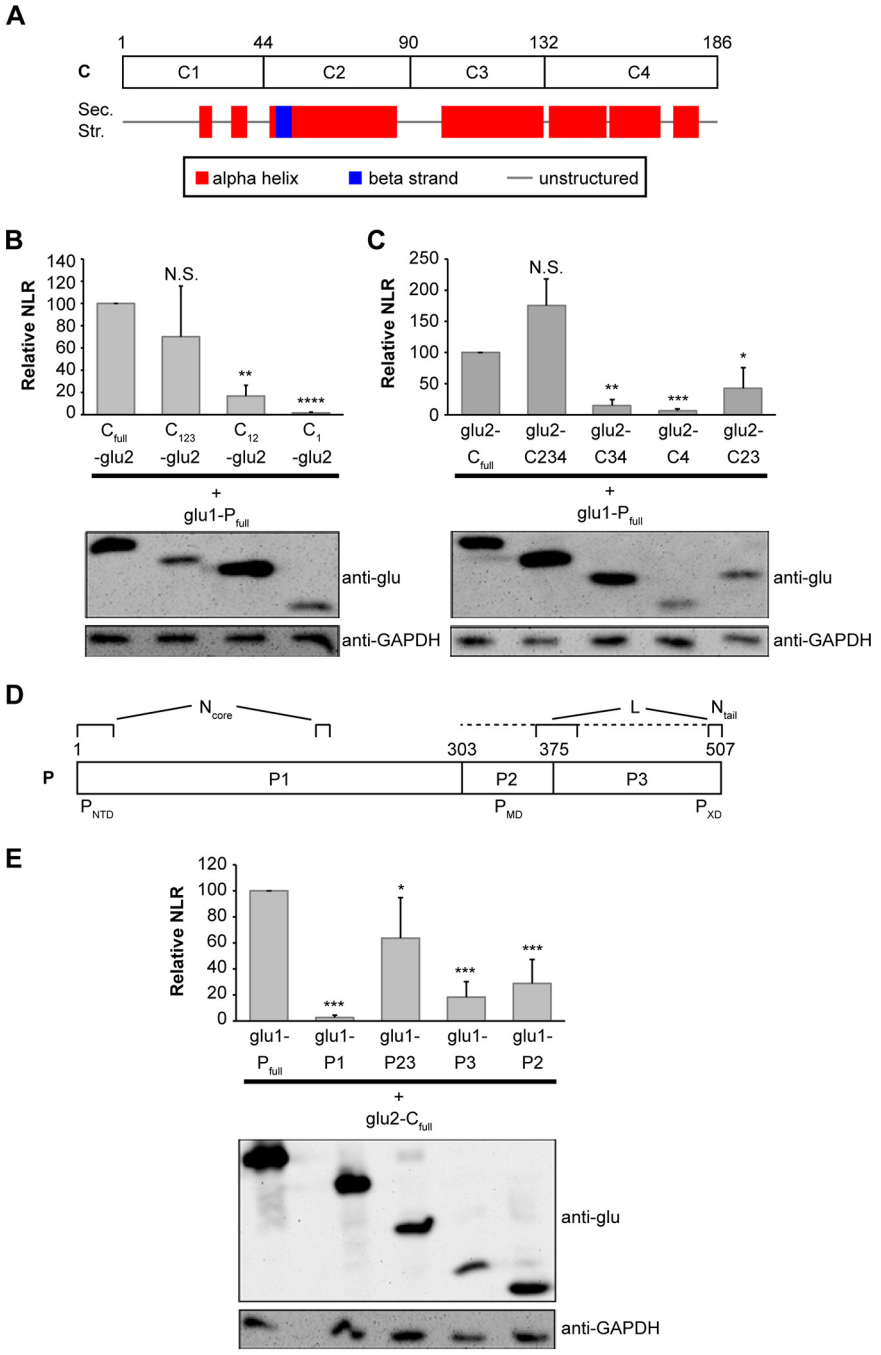

FIG 8 Interacting segments of C and P. (A) Schematic representation of C protein and of the four segments C1 to C4 (white boxes). Predicted secondary structure elements (Sec. str.) are indicated as red (alpha helices) or blue boxes (beta strands) underneath. (B and C) *Gaussia* luciferase-based protein complementation assays of interactions between full-length P protein and carboxy- or amino-terminally truncated C proteins. The normalized luminescence ratio (NLR; vertical axis) is indicated as a percentage of the control interaction with full-length proteins. The proteins used are indicated below the columns, and their expression was confirmed by Western blot analysis (bottom panels) using anti-*Gaussia* luciferase (glu) and anti-GAPDH as a loading control. (D) Schematic representation of P protein, indicating three functional domains (P1 to P3), known interactions with N and L proteins (top), and locations of certain domains (bottom). (E) Interaction between full-length C protein and truncated P proteins. Expression levels of truncated P proteins were analyzed by Western blotting (bottom panel) using anti-glu and anti-GAPDH as a loading control. The diagrams represent average values ± standard deviations of results from three or more independent experiments. Statistical analysis was performed with an unpaired Student's *t* test with Welch's correction comparing activities of protein fragments to the levels seen with full-length proteins (N.S., not significant; *, $P \leq 0.05$; **, $P \leq 0.005$; ***, $P \leq 0.0005$; ****, $P \leq 0.0001$).

Here, we provide molecular evidence of C association with RNPs. This accounts for its ability to enhance replication accuracy. We show that C localizes to viral replication bodies made of N, P, and L proteins, the sites of viral RNA synthesis (3, 45, 52, 53). Additionally, we show that in infected cells, C protein physically interacts with the viral RNP and can be copurified by density gradient centrifugation or immunoprecipitation. Our data indicate that C is indeed a structural protein that interacts with the viral RNP through the cofactor of the viral polymerase, P. While studies using yeast two-hybrid systems or glutathione *S*-transferase (GST) tag purification did not detect a C-P interaction (52, 54), our sensitive mammalian luciferase reconstitution assay revealed such an interaction.

We found that the C protein interacts with the P2 and P3 segments of P (Fig. 8D), but how does this interaction influence the activity of the polymerase complex? The tetrameric P protein has multiple functions. During transcription, it is required for attachment to and movement of the polymerase on the nucleocapsid. During replication, it also delivers free N protein, which is incorporated into progeny nucleocapsid (2). P2 harbors the tetramerization domain (P_{MD}) that is located within the L-binding region (Fig. 8D, dotted line) (34, 38). The P_{XD} sequence proximal to the carboxy terminus interacts with the carboxy-terminal tail of N (N_{tail}), a process modulating the efficiency of transcription reinitiation at each intergenic junction (28). As suggested by the steeper transcription gradient observed with MeV-C^{KO} (5), C binding may regulate the efficiency of P_{XD} interaction with N and, in particular, with the molecular recognition element N_{MoRE} (28, 29, 55). Since MeV-C^{KO} frequently generates DI RNA (4), C binding may also improve the processivity of the P-L complex. Structural and functional evidence that the four P monomers exhibit asymmetric arrangements and binding to N and L partners of MeV and respiratory syncytial virus has been presented recently (34, 38, 56). Thus, the C protein may regulate the formation and maintenance of this asymmetric complex.

Host factors have been identified that interact, directly or indirectly, with the MeV replication machinery. We have shown that cellular protein WD repeat domain protein 5 (WDR5) is recruited to MeV replication bodies (57). Given that it is normally part of the nuclear histone H3-methyltransferase complex, it is unclear what function WDR5 may have in MeV replication. SHC binding and spindle associated protein 1 (SHCBP1) has also been found to interact with both P and C proteins of MeV (14). However, the relevance of this interaction for viral infections remains unclear. While SHCBP1 knockdown affected the replication of a MeV minireplicon, it did not have any effect on viral RNA synthesis in infections, in contrast to the major impairment observed with MeV-C^{KO} (4, 5, 21).

Textbooks currently describe C as an accessory protein (2, 58, 59), because it is dispensable for MeV replication *in vitro* (8). Our data establish the MeV C protein as a component of the viral replication machinery. Combining these results with previously published data (4, 5, 21), we conclude that C contributes to efficient and processive genome synthesis by interacting with P bound to MeV nucleocapsids.

MATERIALS AND METHODS

Cell lines, viruses, and infections. Cells were kept at 37°C/5% CO_2. Vero cells (CCL-81; ATCC, Manassas, VA) were maintained in Dulbecco's modified Eagle medium (D-MEM; HyClone, GE Healthcare Life Sciences, Logan, UT) supplemented with 5% (vol/vol) fetal bovine serum (FBS; Gibco, Thermo Fisher Scientific, Waltham, MA) and 1× penicillin/streptomycin (Corning Life Sciences, Tewksbury, MA). HeLa cells (CCL-2; ATCC) and HEK-293T/17 cells (CRL-11268; ATCC) were maintained in D-MEM supplemented with 10% (vol/vol) FBS and 1× penicillin/streptomycin. BSR-T7/5 cells (60) stably expressing T7 RNA polymerase and HEK-293T cells used for protein complementation assays (CelluloNet BioBank BB-0033-00072; SFR BioSciences, Lyon France) were maintained in D-MEM supplemented with 10% (vol/vol) FBS, 2 mM L-glutamine, and 10 μg/ml gentamicin. Geneticin (1 mg/ml) was added to BSR-T7 cell medium to select for T7 polymerase expression. Recombinant vaccine lineage MeV vac2$(GFP)_H$ (GenBank accession no. MH144178) and MeV $C^{KO}(GFP)_H$ expressing enhanced green fluorescent protein (GFP) from an additional transcription unit were described previously (61). Generation of recombinant vaccine lineage MeV vac2-2tags expressing 3×FLAG-tagged C protein from an additional transcription unit as well as HA-tagged L protein was described previously (57). Cloning of recombinant vac2-notags is described here. Generation of recombinant viruses and stock production and titration were described previously

(62). Infections were carried out at the indicated multiplicities of infection as described previously (4), and infected cells were incubated at 37°C for the indicated amounts of time.

Plasmids. For transient expression of MeV N, pCAGGS-N (kindly provided by Veronika von Messling, who received it from Urs Schneider [63]) was used. Plasmids generated for this study were pCAGGS-P[C^{KO}], pCAGGS-^{HA}L, pCAGGS-C^{FL}, and pB(+)MVvac2-$C^{KO}(C)_H$ (= vac2-notags). Generation of pB(+)MVvac2-$C^{KO}(C^{FL})_H$-^{HA}L (= vac2-2tags) was described previously (57). Plasmids for protein complementation assays were made by introduction of the sequences of interest in modified plasmid pSPICA-N1 or pSPICA-N2 (27, 29) using InFusion (Promega) cloning. The resulting vectors express proteins of interest fused to split *Gaussia* luciferase domains (glu1 and glu2) through linker sequences as follows: glu(1/2)-GGGGS GGGGS PITSL YKVGG RM-(protein of interest) or (protein of interest)-LDGGG GSGGG GSPIT SLYKK VGGRS-glu(1/2). In addition, tag sequences (HA or FLAG) were introduced into the linker region for truncated protein constructs. pEMC-^{FL}L was built from pEMC-La (62) by addition of a FLAG tag sequence to the amino terminus of L (MAIDY KDDDD KLA-L protein). pCG-^{FL}C was made by digestion of pCG-P (41) with XbaI and SlaI and replacement of the P gene by a sequence coding for FLAG-tagged C protein (MDYKDDDDKM-[C protein]). A sequence for expression of Tom20/HA-tagged P protein (MVGRN SAIAA GVCGA LFIG**A** CI**A**FD RKRRS DPNGG YPYDV PDYAM-[P protein]) was cloned downstream of the T7 promoter into the customized pCIRI vector. The details of the cloning strategies, including those used to produce the oligonucleotides used for PCR amplifications, are available upon request.

Transfections. For transient expression, HEK-293T/17 cells were seeded 24 h prior to transfection in 6-cm-diameter dishes at 1×10^6 cells per dish and transfected using Lipofectamine 3000 (Invitrogen, Thermo Fisher Scientific). pCAGGS-N, pCAGGS-P[C^{KO}], and pCAGGS-C^{FL} were used at 750 ng per dish, pCAGGS-^{HA}L was used at 2.5 μg per dish, and the total amount was adjusted to 4 μg per dish using pCAGGS empty vector. Cells were harvested 24 h posttransfection for downstream assays.

Split-luciferase complementation assay. *Gaussia princeps* luciferase-based complementation assays and data analysis (normalized luminescent ratio [NLR]) were performed according to previously described methods (27). HEK-293T cells were seeded 20 h prior transfection in 96-well plates at 2×10^4 cells per well and transfected using jetPRIME reagent (Polyplus transfection). Cells were lysed, and luciferase activity was measured 24 h posttransfection following the *Renilla* luciferase kit protocol (Promega). NLR was calculated by dividing the luciferase signal obtained for the two chimeric partners by the sum of the luciferase signals measured for each chimeric partner mixed with the other "empty" glu domain. Results were expressed as fold increase with respect to a reference interaction, which was set to 100. The threshold above which a signal is considered positive (3.5 NLR) was reevaluated proportionally to the reference interaction.

Antibodies. Rabbit antisera against MeV N (N_{505}), MeV P (P_{254}), MeV V (V_{CTD}), MeV C amino terminus (C_2), MeV C carboxy terminus (C_{176}), and MeV H (H_{CYT}) were used at a dilution of 1:5,000 (Western blotting) or 1:200 (immunofluorescence) as previously described (41, 64, 65). A rabbit antiserum detecting the common amino terminus of P and V proteins (PV_2) was generated against amino acids 2 to 15 of MeV P/V (sequence [C]AEEQARHVKNGLECI) and used at 1:1,000 in Western blotting. A rabbit antiserum recognizing MeV L (L_{2170}) was raised against a peptide corresponding to amino acids 2170 to 2183 of MeV L (sequence [C]EWYKLVGYSALIKD) and used at 1:1,000 (Western blotting) or 1:100 (immunofluorescence). For immunofluorescence, mouse anti-MeV N (clone 25; a kind gift of F. Wild [66]) was used at a 1:200 dilution. A rabbit antiserum anti-P antibody (67) was used at a dilution of 1:1,000, and a mouse anti-FLAG antibody (FLAG M2; Sigma-Aldrich) was used at 1:200 in immunofluorescence. In immunoprecipitations, anti-N_{505} serum was used at 5 μl per 25 μl magnetic beads. For anti-FLAG immunoprecipitations, anti-FLAG M2 magnetic beads (Sigma-Aldrich) were used. For Western blot analysis, anti-Glu rabbit antibody (New England Biolabs) and anti-GAPDH (anti-glyceraldehyde-3-phosphate dehydrogenase) mouse antibody were used at a dilution of 1:2,000. Anti-mouse horseradish peroxidase (HRP) and anti-rabbit HRP secondary antibodies were used at dilution of 1:5,000. Reagents used for Western blot detection were anti-mouse and anti-rabbit-HRP (Jackson Immunoresearch, West Grove, PA) (1:5,000 to 1:25,000) or HRP protein A (Invitrogen, Thermo Fisher Scientific) (1:10,000). For immunofluorescence, anti-mouse Alexa 405, anti-rabbit Alexa 488, anti-mouse Alexa 555, and anti-rabbit Alexa 647 (all from Molecular Probes, Eugene, OR) were used at a 1:200 to 1:750 dilution. Actin was stained with Alexa 594-conjugated phalloidin (Molecular Probes) at a 1:40 dilution.

Immunofluorescence staining. HeLa cells were seeded in 35-mm-diameter cell imaging dishes with 170-μm-thick glass bottoms (Eppendorf, Hamburg, Germany) at 1×10^5 cells per dish 18 h prior to infection and were later infected at a multiplicity of infection of 0.1. Cells were washed with phosphate-buffered saline (PBS) once at 48 h postinfection and fixed with fixation reagent containing 4% paraformaldehyde (Santa Cruz Biotechnology, Dallas TX) for 15 min at room temperature. Cells were then permeabilized with 0.1% (vol/vol) Triton X-100–PBS for 5 min at room temperature and incubated with blocking reagent containing 10% (wt/vol) normal goat serum and 1% (wt/vol) bovine serum albumin (BSA)–PBS for 30 min. Cells were incubated with primary antibodies at the dilutions indicated above in blocking solution for 2 h at room temperature on a rocking platform, followed by three wash steps with PBS. Incubation with secondary antibodies diluted in blocking solution was carried out for 1 h at room temperature, followed by three wash steps with PBS and two additional wash steps with deionized H_2O. Cells were overlaid with ProLong Gold antifade mountant (Molecular Probes), and microscopy was carried out on a laser scanning microscope (LSM) (model LSM 780; Carl Zeiss Microscopy, Jena, Germany) using a 40× objective (Carl Zeiss Microscopy) (C-Apochromat 40×/1.20 W Korr M27, 2.5× zoom). Image processing and analysis were performed with ZEN 2.1 Black Edition software (version 11.0; Carl Zeiss Microscopy) and Adobe Photoshop CC (release 2017.0.1; Adobe Systems Inc., San Jose, CA).

For Tom20 assays, BSR-T7/5 cells were seeded into Lab-Tek plates (Iwaki) (0.7×10^5 cells/well) and transfected 20 h later with 400 ng plasmid using jetPRIME reagent (Polyplus transfection). In these cells, stably expressed T7 RNA polymerase allows expression of ^{FL}L protein from the T7 promoter-driven pEMC-^{FL}L plasmid. At 24 h posttransfection, the cells were fixed in 4% formaldehyde for 30 min at room temperature and then washed 3 times with PBS prior saturation followed by permeabilization in PBS containing 4% fetal bovine serum (FBS) and 0.3% Triton X-100 (PBS-FBS-Triton buffer). Primary antibodies were diluted in PBS-FBS-Triton buffer and incubated on the cells overnight at 4°C. The cells were then washed four times and incubated with 4′,6-diamidino-2-phenylindole (DAPI; 1:1,000) and both anti-mouse and anti-rabbit secondary antibodies. After four washes, slides were mounted with Fluoprep mounting medium (bioMérieux catalog no.75521). Microscopy was carried out on a LSM 710 confocal microscope (Carl Zeiss Microscopy, Jena, Germany). Image processing and analysis were performed using ImageJ software.

Immunoprecipitation (IP). Infected cells were harvested at the indicated time points. Cells were washed once with PBS, resuspended in ice-cold Co-IP buffer (50 mM Tris [pH 7.5], 150 mM NaCl, 2 mM EDTA, 1 mM sodium orthovanadate, 0.5% [vol/vol] NP-40 substitute) with protease inhibitor cocktail (Roche Diagnostics, Indianapolis, IN), and lysed for 15 min on a rotating platform. Nuclei were pelleted by centrifugation (20,000 × *g*, 15 min, 4°C), and supernatants were filtered through a 0.2-μm-pore-size syringe filter. The cleared lysates (100 μl) were collected for input analysis and stored at −20°C. For anti-FLAG IP, the remaining lysates were incubated with 25 μl anti-FLAG M2 magnetic beads (Sigma-Aldrich) for 3 h at 4°C on a rotating platform. After incubation, beads were collected on a magnetic stand and the lysate was discarded. Beads were washed three times with Co-IP buffer, and bound proteins were eluted using 3×FLAG peptide (Sigma-Aldrich) at a concentration of 150 μg/ml in 100 μl Co-IP buffer. Samples were stored at −20°C. For other immunoprecipitations, magnetic beads (Pierce Crosslink Magnetic IP/Co-IP kit; Thermo Fisher Scientific) were coated with anti-N_{505} serum (5 μl serum per 25 μl beads) and cross-linked according to the manual. Beads were incubated with lysates and washed as described above. Immunoprecipitated proteins were eluted using acid washing as described in the manual.

RNP preparation. MeV RNPs were purified by CsCl density gradient ultracentrifugation as described previously (21). Thirty dishes (150-mm diameter) of HeLa cells were infected with MeV at multiplicity of infection of 0.1 for 72 h. At the time of harvest, cells from 10 dishes each were collected and lysed in 3 ml lysis buffer with 0.65% (vol/vol) NP-40. Ultracentrifugation was carried out in SW41 tubes (Beckman-Coulter) with an approximate total volume of 11 ml loaded with the following (top to bottom): 5 ml cell lysate, 1 ml 5% (wt/vol) sucrose buffer, 1.5 ml 25% (wt/vol) CsCl buffer, 2.5 ml 30% (wt/vol) CsCl buffer, and 1 ml 40% (wt/vol) CsCl buffer. Various amounts of sarkosyl were added to the buffers for each preparation. After the first centrifugation step, the top 1-ml fraction containing soluble proteins ("supernatant") and the visible RNP bands floating within the CsCl gradient (1 to 2 ml volume) were extracted. The RNP fractions were then precipitated through LEH buffer (100 mM LiCl, 1 mM EDTA, 10 mM HEPES, pH 7.5), and pellets ("purified RNP") were resuspended in LEH buffer supplemented with 1% (wt/vol) SDS for direct Western blot analysis. The supernatant and the RNP solutions were stored at −80°C.

Western blot analysis. For detection of C and C^{FL}, samples were separated on 16% SDS gels. For detection of N and P, samples were separated on 10% SDS gels, and for detection of L and ^{HA}L, samples were separated on 6% SDS gels. Protein samples were subjected to heat denaturing in a buffer containing 4 M urea. Gels were transferred to polyvinylidene difluoride (PVDF) membranes (Immobilon-P, EMD Millipore) for 2 h at 400 mA using a wet transfer system (Bio-Rad, Hercules, CA). Membranes were incubated in blocking solution (5% [wt/vol] nonfat dry milk–Tris-buffered saline [TBS] or bovine serum albumin fraction V [BSA]–TBS) for 1 h at room temperature and further incubated with primary antibodies at the dilutions indicated above in blocking solution supplemented with 1:2,000 Tween 20. Incubation was carried out overnight at 4°C on a rocking platform. After three washes with TBS–0.5% (vol/vol) Tween 20 (TBST), membranes were incubated with secondary antibodies in TBST for 1 h at room temperature, washed again three times, and then incubated with ECL substrate (Supersignal Western Pico; Pierce, Thermo Fisher Scientific) for 5 min at room temperature. Membranes were scanned using a ChemiDoc imaging system (Bio-Rad) and analyzed using Image Lab software (v 6.0.0 build 25; Bio-Rad).

Silver staining. RNP samples were fractionated on 4%-to-20%-gradient SDS gels (Bio-Rad) and fixed in fixative solution (50% [vol/vol] methanol, 10% [vol/vol] acetic acid) for 30 min at room temperature. The gel was then washed once with 5% (vol/vol) methanol for 15 min and three times with Nanopure H_2O for 5 min. The gel was then washed with sensitizing reagent (0.02% [wt/vol] sodium thiosulfate) solution for 2 min, followed by two washes with Nanopure H_2O for 30 s each time. Next, the gel was incubated in 0.15% (wt/vol) silver nitrate solution for 60 min at room temperature and then washed once in Nanopure H_2O for 1 min and in 3% (wt/vol) sodium carbonate solution for 1 min. Finally, the gel was developed by incubation with 100 ml developer solution (3% [wt/vol] sodium carbonate supplemented with 2 ml sensitizing reagent and 50 μl formaldehyde) until bands became visible. Development was stopped by exchanging the buffer to 1.4% (wt/vol) EDTA solution. Images were captured using a GelDoc XR+ imager with a transillumination screen (Bio-Rad) and processed using Image Lab software (v 6.0.0, build 25; Bio-Rad).

ACKNOWLEDGMENTS

We thank Patricia Devaux, Alex Generous, and Chanakha K. Navaratnarajah for their valuable input in discussing the data and manuscript. Patricia Devaux, Veronika von Messling, and Friedemann Weber kindly provided plasmids.

R.C.D., A.L.H., W.P.B., I.Y., S.C., A.J.S., and A.J.M. were supported by fellowships of the Mayo Clinic Graduate School of Biomedical Sciences (MCGSBS). This work was supported by NIH grant R21-AI128037-01. The funders had no role in study design, data collection and interpretation, or the decision to submit the work for publication.

REFERENCES

1. Pfaller CK, Cattaneo R, Schnell MJ. 2015. Reverse genetics of Mononegavirales: how they work, new vaccines, and new cancer therapeutics. Virology 479-480:331–344. https://doi.org/10.1016/j.virol.2015.01.029.
2. Lamb RA, Parks GD. 2013. Paramyxoviridae, p 957–995. *In* Knipe DM, Howley PM, Howley PM, Cohen JI, Griffin DE, Lamb RA, Martin MA, Racaniello VR, Roizman B (ed), Fields virology, 6th ed, vol 1. Lippincott Williams & Wilkins, Philadelphia, PA.
3. Bellini WJ, Englund G, Rozenblatt S, Arnheiter H, Richardson CD. 1985. Measles virus P gene codes for two proteins. J Virol 53:908–919.
4. Pfaller CK, Mastorakos GM, Matchett WE, Ma X, Samuel CE, Cattaneo R. 2015. Measles virus defective interfering RNAs are generated frequently and early in the absence of C protein and can be destabilized by adenosine deaminase acting on RNA-1-like hypermutations. J Virol 89:7735–7747. https://doi.org/10.1128/JVI.01017-15.
5. Pfaller CK, Radeke MJ, Cattaneo R, Samuel CE. 2014. Measles virus C protein impairs production of defective copyback double-stranded viral RNA and activation of protein kinase R. J Virol 88:456–468. https://doi.org/10.1128/JVI.02572-13.
6. Runge S, Sparrer KM, Lassig C, Hembach K, Baum A, Garcia-Sastre A, Soding J, Conzelmann KK, Hopfner KP. 2014. In vivo ligands of MDA5 and RIG-I in measles virus-infected cells. PLoS Pathog 10:e1004081. https://doi.org/10.1371/journal.ppat.1004081.
7. Mura M, Combredet C, Najburg V, Sanchez David DRY, Tangy F, Komarova AV. 2017. Nonencapsidated 5′ copy-back defective interfering genomes produced by recombinant measles viruses are recognized by RIG-I and LGP2 but not MDA5. J Virol 91:e00643-17.
8. Radecke F, Billeter MA. 1996. The nonstructural C protein is not essential for multiplication of Edmonston B strain measles virus in cultured cells. Virology 217:418–421. https://doi.org/10.1006/viro.1996.0134.
9. Takeuchi K, Takeda M, Miyajima N, Ami Y, Nagata N, Suzaki Y, Shahnewaz J, Kadota S, Nagata K. 2005. Stringent requirement for the C protein of wild-type measles virus for growth both in vitro and in macaques. J Virol 79:7838–7844. https://doi.org/10.1128/JVI.79.12.7838-7844.2005.
10. Escoffier C, Manie S, Vincent S, Muller CP, Billeter M, Gerlier D. 1999. Nonstructural C protein is required for efficient measles virus replication in human peripheral blood cells. J Virol 73:1695–1698.
11. Devaux P, Hodge G, McChesney MB, Cattaneo R. 2008. Attenuation of V- or C-defective measles viruses: infection control by the inflammatory and interferon responses of rhesus monkeys. J Virol 82:5359–5367. https://doi.org/10.1128/JVI.00169-08.
12. Reutter GL, Cortese-Grogan C, Wilson J, Moyer SA. 2001. Mutations in the measles virus C protein that up regulate viral RNA synthesis. Virology 285:100–109. https://doi.org/10.1006/viro.2001.0962.
13. Bankamp B, Wilson J, Bellini WJ, Rota PA. 2005. Identification of naturally occurring amino acid variations that affect the ability of the measles virus C protein to regulate genome replication and transcription. Virology 336:120–129. https://doi.org/10.1016/j.virol.2005.03.009.
14. Ito M, Iwasaki M, Takeda M, Nakamura T, Yanagi Y, Ohno S. 2013. Measles virus nonstructural C protein modulates viral RNA polymerase activity by interacting with host protein SHCBP1. J Virol 87:9633–9642. https://doi.org/10.1128/JVI.00714-13.
15. Giraudon P, Gerald C, Wild TF. 1984. A study of measles virus antigens in acutely and persistently infected cells using monoclonal antibodies: differences in the accumulation of certain viral proteins. Intervirology 21:110–120. https://doi.org/10.1159/000149509.
16. Zhou Y, Su JM, Samuel CE, Ma D. 2019. Measles virus forms inclusion bodies with properties of liquid organelles. J Virol 93:e00948-19.
17. Sparrer KM, Pfaller CK, Conzelmann KK. 2012. Measles virus C protein interferes with beta interferon transcription in the nucleus. J Virol 86:796–805. https://doi.org/10.1128/JVI.05899-11.
18. Cattaneo R, Kaelin K, Baczko K, Billeter MA. 1989. Measles virus editing provides an additional cysteine-rich protein. Cell 56:759–764. https://doi.org/10.1016/0092-8674(89)90679-x.
19. Guryanov SG, Liljeroos L, Kasaragod P, Kajander T, Butcher SJ. 2015. Crystal structure of the measles virus nucleoprotein core in complex with an N-terminal region of phosphoprotein. J Virol 90:2849–2857. https://doi.org/10.1128/JVI.02865-15.
20. Milles S, Jensen MR, Lazert C, Guseva S, Ivashchenko S, Communie G, Maurin D, Gerlier D, Ruigrok RWH, Blackledge M. 2018. An ultraweak interaction in the intrinsically disordered replication machinery is essential for measles virus function. Sci Adv 4:eaat7778. https://doi.org/10.1126/sciadv.aat7778.
21. Pfaller CK, Donohue RC, Nersisyan S, Brodsky L, Cattaneo R. 2018. Extensive editing of cellular and viral double-stranded RNA structures accounts for innate immunity suppression and the pro-viral activity of ADAR1p150. PLoS Biol 16:e2006577. https://doi.org/10.1371/journal.pbio.2006577.
22. Udem SA, Cook KA. 1984. Isolation and characterization of measles virus intracellular nucleocapsid RNA. J Virol 49:57–65.
23. Huber M, Cattaneo R, Spielhofer P, Orvell C, Norrby E, Messerli M, Perriard JC, Billeter MA. 1991. Measles virus phosphoprotein retains the nucleocapsid protein in the cytoplasm. Virology 185:299–308. https://doi.org/10.1016/0042-6822(91)90777-9.
24. Horikami SM, Smallwood S, Bankamp B, Moyer SA. 1994. An amino-proximal domain of the L protein binds to the P protein in the measles virus RNA polymerase complex. Virology 205:540–545. https://doi.org/10.1006/viro.1994.1676.
25. Hulett JM, Lueder F, Chan NC, Perry AJ, Wolynec P, Likic VA, Gooley PR, Lithgow T. 2008. The transmembrane segment of Tom20 is recognized by Mim1 for docking to the mitochondrial TOM complex. J Mol Biol 376:694–704. https://doi.org/10.1016/j.jmb.2007.12.021.
26. Kanaji S, Iwahashi J, Kida Y, Sakaguchi M, Mihara K. 2000. Characterization of the signal that directs Tom20 to the mitochondrial outer membrane. J Cell Biol 151:277–288. https://doi.org/10.1083/jcb.151.2.277.
27. Cassonnet P, Rolloy C, Neveu G, Vidalain PO, Chantier T, Pellet J, Jones L, Muller M, Demeret C, Gaud G, Vuillier F, Lotteau V, Tangy F, Favre M, Jacob Y. 2011. Benchmarking a luciferase complementation assay for detecting protein complexes. Nat Methods 8:990–992. https://doi.org/10.1038/nmeth.1773.
28. Bloyet LM, Brunel J, Dosnon M, Hamon V, Erales J, Gruet A, Lazert C, Bignon C, Roche P, Longhi S, Gerlier D. 2016. Modulation of re-initiation of measles virus transcription at intergenic regions by PXD to NTAIL binding strength. PLoS Pathog 12:e1006058. https://doi.org/10.1371/journal.ppat.1006058.
29. Brunel J, Chopy D, Dosnon M, Bloyet LM, Devaux P, Urzua E, Cattaneo R, Longhi S, Gerlier D. 2014. Sequence of events in measles virus replication: role of phosphoprotein-nucleocapsid interactions. J Virol 88:10851–10863. https://doi.org/10.1128/JVI.00664-14.
30. Communie G, Crepin T, Maurin D, Jensen MR, Blackledge M, Ruigrok RW. 2013. Structure of the tetramerization domain of measles virus phosphoprotein. J Virol 87:7166–7169. https://doi.org/10.1128/JVI.00487-13.
31. Bankamp B, Horikami SM, Thompson PD, Huber M, Billeter M, Moyer SA. 1996. Domains of the measles virus N protein required for binding to P protein and self-assembly. Virology 216:272–277. https://doi.org/10.1006/viro.1996.0060.
32. Harty RN, Palese P. 1995. Measles virus phosphoprotein (P) requires the NH2- and COOH-terminal domains for interactions with the nucleoprotein (N) but only the COOH terminus for interactions with itself. J Gen Virol 76:2863–2867. https://doi.org/10.1099/0022-1317-76-11-2863.
33. Poch O, Blumberg BM, Bougueleret L, Tordo N. 1990. Sequence comparison of five polymerases (L proteins) of unsegmented negative-strand RNA viruses: theoretical assignment of functional domains. J Gen Virol 71:1153–1162. https://doi.org/10.1099/0022-1317-71-5-1153.
34. Bloyet LM, Schramm A, Lazert C, Raynal B, Hologne M, Walker O, Longhi S, Gerlier D. 2019. Regulation of measles virus gene expression by P protein coiled-coil properties. Sci Adv 5:eaaw3702. https://doi.org/10.1126/sciadv.aaw3702.
35. Lo MK, Sogaard TM, Karlin DG. 2014. Evolution and structural organization of the C proteins of paramyxovirinae. PLoS One 9:e90003. https://doi.org/10.1371/journal.pone.0090003.

36. Blocquel D, Habchi J, Durand E, Sevajol M, Ferron F, Erales J, Papageorgiou N, Longhi S. 2014. Coiled-coil deformations in crystal structures: the measles virus phosphoprotein multimerization domain as an illustrative example. Acta Crystallogr D Biol Crystallogr 70:1589–1603. https://doi.org/10.1107/S139900471400234X.
37. Longhi S, Bloyet LM, Gianni S, Gerlier D. 2017. How order and disorder within paramyxoviral nucleoproteins and phosphoproteins orchestrate the molecular interplay of transcription and replication. Cell Mol Life Sci 74:3091–3118. https://doi.org/10.1007/s00018-017-2556-3.
38. Du Pont V, Jiang Y, Plemper RK. 2019. Bipartite interface of the measles virus phosphoprotein X domain with the large polymerase protein regulates viral polymerase dynamics. PLoS Pathog 15:e1007995. https://doi.org/10.1371/journal.ppat.1007995.
39. Lamb RA, Choppin PW. 1978. Determination by peptide mapping of the unique polypeptides in Sendai virions and infected cells. Virology 84:469–478. https://doi.org/10.1016/0042-6822(78)90263-5.
40. Dethlefsen L, Kolakofsky D. 1983. In vitro synthesis of the nonstructural C protein of Sendai virus. J Virol 46:321–324.
41. Devaux P, Cattaneo R. 2004. Measles virus phosphoprotein gene products: conformational flexibility of the P/V protein amino-terminal domain and C protein infectivity factor function. J Virol 78:11632–11640. https://doi.org/10.1128/JVI.78.21.11632-11640.2004.
42. Kurotani A, Kiyotani K, Kato A, Shioda T, Sakai Y, Mizumoto K, Yoshida T, Nagai Y. 1998. Sendai virus C proteins are categorically nonessential gene products but silencing their expression severely impairs viral replication and pathogenesis. Genes Cells 3:111–124. https://doi.org/10.1046/j.1365-2443.1998.00170.x.
43. Nagai Y, Kato A. 2004. Accessory genes of the paramyxoviridae, a large family of nonsegmented negative-strand RNA viruses, as a focus of active investigation by reverse genetics. Curr Top Microbiol Immunol 283:197–248. https://doi.org/10.1007/978-3-662-06099-5_6.
44. Fontana JM, Bankamp B, Bellini WJ, Rota PA. 2008. Regulation of interferon signaling by the C and V proteins from attenuated and wild-type strains of measles virus. Virology 374:71–81. https://doi.org/10.1016/j.virol.2007.12.031.
45. Nakatsu Y, Takeda M, Ohno S, Shirogane Y, Iwasaki M, Yanagi Y. 2008. Measles virus circumvents the host interferon response by different actions of the C and V proteins. J Virol 82:8296–8306. https://doi.org/10.1128/JVI.00108-08.
46. Oda K, Matoba Y, Irie T, Kawabata R, Fukushi M, Sugiyama M, Sakaguchi T. 2015. Structural basis of the inhibition of STAT1 activity by Sendai virus C protein. J Virol 89:11487–11499. https://doi.org/10.1128/JVI.01887-15.
47. Shaffer JA, Bellini WJ, Rota PA. 2003. The C protein of measles virus inhibits the type I interferon response. Virology 315:389–397. https://doi.org/10.1016/S0042-6822(03)00537-3.
48. Takeuchi K, Komatsu T, Yokoo J, Kato A, Shioda T, Nagai Y, Gotoh B. 2001. Sendai virus C protein physically associates with Stat1. Genes Cells 6:545–557. https://doi.org/10.1046/j.1365-2443.2001.00442.x.
49. Horikami SM, Hector RE, Smallwood S, Moyer SA. 1997. The Sendai virus C protein binds the L polymerase protein to inhibit viral RNA synthesis. Virology 235:261–270. https://doi.org/10.1006/viro.1997.8702.
50. Irie T, Okamoto I, Yoshida A, Nagai Y, Sakaguchi T. 2014. Sendai virus C proteins regulate viral genome and antigenome synthesis to dictate the negative genome polarity. J Virol 88:690–698. https://doi.org/10.1128/JVI.02798-13.
51. Boonyaratanakornkit J, Bartlett E, Schomacker H, Surman S, Akira S, Bae YS, Collins P, Murphy B, Schmidt A. 2011. The C proteins of human parainfluenza virus type 1 limit double-stranded RNA accumulation that would otherwise trigger activation of MDA5 and protein kinase R. J Virol 85:1495–1506. https://doi.org/10.1128/JVI.01297-10.
52. Iwasaki M, Takeda M, Shirogane Y, Nakatsu Y, Nakamura T, Yanagi Y. 2009. The matrix protein of measles virus regulates viral RNA synthesis and assembly by interacting with the nucleocapsid protein. J Virol 83:10374–10383. https://doi.org/10.1128/JVI.01056-09.
53. Nakatsu Y, Ma X, Seki F, Suzuki T, Iwasaki M, Yanagi Y, Komase K, Takeda M. 2013. Intracellular transport of the measles virus ribonucleoprotein complex is mediated by Rab11A-positive recycling endosomes and drives virus release from the apical membrane of polarized epithelial cells. J Virol 87:4683–4693. https://doi.org/10.1128/JVI.02189-12.
54. Liston P, DiFlumeri C, Briedis DJ. 1995. Protein interactions entered into by the measles virus P, V, and C proteins. Virus Res 38:241–259. https://doi.org/10.1016/0168-1702(95)00067-Z.
55. Bourhis JM, Receveur-Brechot V, Oglesbee M, Zhang X, Buccellato M, Darbon H, Canard B, Finet S, Longhi S. 2005. The intrinsically disordered C-terminal domain of the measles virus nucleoprotein interacts with the C-terminal domain of the phosphoprotein via two distinct sites and remains predominantly unfolded. Protein Sci 14:1975–1992. https://doi.org/10.1110/ps.051411805.
56. Gilman MSA, Liu C, Fung A, Behera I, Jordan P, Rigaux P, Ysebaert N, Tcherniuk S, Sourimant J, Eleouet JF, Sutto-Ortiz P, Decroly E, Roymans D, Jin Z, McLellan JS. 2019. Structure of the respiratory syncytial virus polymerase complex. Cell 179:193–204.e14. https://doi.org/10.1016/j.cell.2019.08.014.
57. Ma D, George CX, Nomburg J, Pfaller CK, Cattaneo R, Samuel CE. 2018. Upon infection, cellular WD repeat-containing protein 5 (WDR5) localizes to cytoplasmic inclusion bodies and enhances measles virus replication. J Virol 92:e01726-17. https://doi.org/10.1128/JVI.01726-17.
58. Griffin DE. 2013. Measles virus, p 1042–1069. *In* Knipe DM, Howley PM, Cohen JI, Griffin DE, Lamb RA, Martin MA, Racaniello VR, Roizman B (ed), Fields virology, 6th ed, vol 1. Lippincott Williams & Wilkins, Philadelphia, PA.
59. Whelan S. 2013. Viral replication strategies, p 105–126. *In* Knipe DM, Howley PM, Cohen JI, Griffin DE, Lamb RA, Martin MA, Racaniello VR, Roizman B (ed), Fields virology, 6th ed, vol 1. Lippincott Williams & Wilkins, Philadelphia, PA.
60. Finke S, Conzelmann KK. 1999. Virus promoters determine interference by defective RNAs: selective amplification of mini-RNA vectors and rescue from cDNA by a 3′ copy-back ambisense rabies virus. J Virol 73:3818–3825.
61. Devaux P, von Messling V, Songsungthong W, Springfeld C, Cattaneo R. 2007. Tyrosine 110 in the measles virus phosphoprotein is required to block STAT1 phosphorylation. Virology 360:72–83. https://doi.org/10.1016/j.virol.2006.09.049.
62. Radecke F, Spielhofer P, Schneider H, Kaelin K, Huber M, Dotsch C, Christiansen G, Billeter MA. 1995. Rescue of measles viruses from cloned DNA. EMBO J 14:5773–5784. https://doi.org/10.1002/j.1460-2075.1995.tb00266.x.
63. Martin A, Staeheli P, Schneider U. 2006. RNA polymerase II-controlled expression of antigenomic RNA enhances the rescue efficacies of two different members of the Mononegavirales independently of the site of viral genome replication. J Virol 80:5708–5715. https://doi.org/10.1128/JVI.02389-05.
64. Cathomen T, Naim HY, Cattaneo R. 1998. Measles viruses with altered envelope protein cytoplasmic tails gain cell fusion competence. J Virol 72:1224–1234.
65. Toth AM, Devaux P, Cattaneo R, Samuel CE. 2009. Protein kinase PKR mediates the apoptosis induction and growth restriction phenotypes of C protein-deficient measles virus. J Virol 83:961–968. https://doi.org/10.1128/JVI.01669-08.
66. Giraudon P, Wild TF. 1981. Monoclonal antibodies against measles virus. J Gen Virol 54:325–332. https://doi.org/10.1099/0022-1317-54-2-325.
67. Chen M, Cortay JC, Logan IR, Sapountzi V, Robson CN, Gerlier D. 2005. Inhibition of ubiquitination and stabilization of human ubiquitin E3 ligase PIRH2 by measles virus phosphoprotein. J Virol 79:11824–11836. https://doi.org/10.1128/JVI.79.18.11824-11836.2005.